Advances in Applied Mathematics and Mechanics
Adv. Appl. Math. Mech., Vol. **2**, No. 6, pp. 701-721

DOI: 10.4208/aamm.09-m0993
December 2010

On the Full C_1-Q_k Finite Element Spaces on Rectangles and Cuboids

Shangyou Zhang*

[1] *Department of Mathematical Sciences, University of Delaware, Newark, Delaware 19716-2553, USA*

Received 14 October 2009; Accepted (in revised version) 21 June 2010
Available online 26 August 2010

Abstract. We study the extensions of the Bogner-Fox-Schmit element to the whole family of Q_k continuously differentiable finite elements on rectangular grids, for all $k \geq 3$, in 2D and 3D. We show that the newly defined C_1 spaces are maximal in the sense that they contain all C_1-Q_k functions of piecewise polynomials. We give examples of other extensions of C_1-Q_k elements. The result is consistent with the Strang's conjecture (restricted to the quadrilateral grids in 2D and 3D). Some numerical results are provided on the family of C_1 elements solving the biharmonic equation.

AMS subject classifications: 65M60, 65N30

Key words: Differentiable finite element, biharmonic equation, Bogner-Fox-Schmit rectangle, quadrilateral element, hexahedral element, Strang's conjecture.

---

1 Introduction

It is relatively difficult to construct continuously-differentiable finite elements in two and three space dimensions. Most such C_1 elements were designed in 1970s and earlier (cf. Ciarlet [10]). Most C_1 elements were constructed on triangles and tetrahedra with piecewise polynomials P_k. As usual, P_k and Q_k stand for polynomials of total degree and separate degree k or less, respectively. For example, we have the Argyris P_5-triangle (1968), the Bell reduced P_5-triangle (1969), the Morgan-Scott P_k-triangles ($k \geq 5$) (1975), the Hsieh-Clough-Tocher P_3-macrotriangles (1965), the reduced Hsieh-Clough-Tocher P_3-macrotriangles (1976), the Douglass-Dupont-Percell-Scott P_k-triangles (1979), the Powell-Sabin P_2-triangles (1977), the Fraeijs de Veubeke-Sander P_3 quadrilateral and its reduced version (1964), cf. [2,4,10–12,14,15,22,25,27,28,37]. The

*Corresponding author.
URL: `http://www.math.udel.edu/~szhang/`
Email: szhang@udel.edu (S. Y. Zhang)

last two elements carry the term quadrilateral in the name, but they are P_k macrotriangle elements too. It seems that the Bogner-Fox-Schmit rectangle (1965) is the only C_1 element on rectangular grids, cf. [9,10]. Nevertheless, there are still quite some work on this one of the oldest elements, mainly due to its simplicity and effectiveness in computation, cf. [1,20,24,26].

In this paper, we study the Bogner-Fox-Schmit element extended to higher order Q_k elements in 2D and 3D, $k\geq 3$. Such extensions were done also in [8,13,21]. There might not be much interest in application to use high order elements, though they provide usually a better accuracy with less number of unknowns. For example, as shown in our numerical tests, the Q_4 element performs better than its Q_3 cousin, the Bogner-Fox-Schmit element. However, our main interest in studying C_1-Q_k elements is to understand the structure and approximation property of C_0-Q_{k-1} element under the divergence-free or the nearly-incompressible constraint, cf. two subsequent researches [38,39]. The approach is standard. Morgan and Scott [22] modified Argyris P_5-triangles to cover all C_1-P_5 functions on triangular grids, and extended it to C_1-P_k for all $k\geq 5$. Scott and Vogelius [29,30] showed that C_0-P_k elements for all $k\geq 4$ provide the optimal-order approximation property on general triangular grids under the incompressibility constraint, for fluids and elasticity. The generalization of Scott and Vogelius work to Q_k polynomials is not accomplished yet. There are some work on Q_k elements under the incompressibility constraint and the element is shown suboptimal, cf. [3,32].

The construction of high-order C_1 finite elements is relatively easy, compared with that of low-order elements. Such a construction consists of two parts, the local uniqueness and polynomial preserving, and the global inter-element coupling. We note that Gopalacharyulu made an extension to the Bogner-Fox-Schmit element in [17]. The extension is not a higher order element, but an element which includes some higher order polynomial terms so that the element may work better for plates. Our work here extends the element of Gopalacharyulu, so that the higher order approximation can be guaranteed. In fact, it was pointed out by Watkins that the construction of Gopalacharyulu missed some lower order terms while adding higher order terms to the Bogner-Fox-Schmit element, cf. [36]. To correct it, Gopalacharyulu added some more terms into the element, however, without showing the extension is conforming (C_1), neither complete, in [18]. For the extensions studied in this paper, we show their completeness (the optimal order of approximation), fullness (including all C_1-Q_k polynomials), and conformity. This is mainly the work further that of [8,13,21].

For C_1 piecewise polynomials on triangular grids, Strang gave a conjecture on the dimension based on the inter-element constraint, cf. [5,23,33,34]. The conditions and validity of the Strang's conjecture are open problems, cf. [23]. But we will show the conjecture holds on rectangular grids, both in 2D and 3D.

The paper has three additional sections. In Section 2, 2D C_1-Q_k elements are constructed for all $k\geq 3$. In Section 3, 3D C_1-Q_k elements are constructed for all $k\geq 3$. In Section 4, a simple numerical test on the biharmonic equation is performed with the Bogner-Fox-Schmit element and higher order C_1-Q_k elements.

2 Families of C_1-Q_k elements on rectangular grids

In this section, we will review the construction of the Bogner-Fox-Schmit element, and its basis functions. We will extend it to finite elements of higher degree polynomials. We will show the finite element space is full that it includes all C_1-Q_k piecewise polynomials. Some examples of partial coverage will be given. Also an example of natural extension, which contradicts the Strang's conjecture, will be shown to fail to produce C_1 elements.

Let Ω be a polygonal domain in 2D and 3D which can be discretized into rectangles and cuboids (rectangular boxes) parallel to the coordinate planes, denoted by Ω_h. For simplicity, we may let Ω be the unit square or the unit cube with the uniform grid of size h (=$1/N$):

$$\Omega_h = \begin{cases} \cup_{1\le i,j\le N}\Omega_{ij}, & \text{in 2D},\\ \cup_{1\le i,j,l\le N}\Omega_{ijl}, & \text{in 3D}, \end{cases} \tag{2.1}$$

where

$$\begin{aligned} \Omega_{ij} &= \big\{(x,y) \mid (i-1)h \le x \le ih, \ \ (j-1)h \le y \le jh\big\},\\ \Omega_{ijl} &= \big\{(x,y,z) \mid (i-1)h \le x \le ih, \ \ (j-1)h \le y \le jh, \ \ (l-1)h \le z \le lh\big\}. \end{aligned}$$

As usual, polynomial spaces are denoted by (similarly in 2D too)

$$\begin{aligned} P_k &= \Big\{p(x,y,z) \mid p(x,y,z) = \sum_{0\le i+j+l\le k} c_{ijl}x^iy^jz^l\Big\},\\ Q_k &= \Big\{p(x,y,z) \mid p(x,y,z) = \sum_{0\le i,j,l\le k} c_{ijl}x^iy^jz^l\Big\}. \end{aligned}$$

For example

$$P_1 = \operatorname{span}\{1,x,y,z\} \quad \text{and} \quad Q_1 = \operatorname{span}\{1,x,y,z,xy,xz,yz,xyz\}.$$

The C_1-Q_k finite element spaces on Ω_h are defined by

$$V_k = \Big\{v \in C_1(\Omega)\Big|\ v|_{\Omega_{ijl}} \in Q_k, \quad \forall\Omega_{ijl} \in \Omega_h\Big\}, \tag{2.2a}$$

$$V_{k,0} = \Big\{v \in V_k\Big|\ v|_{\partial\Omega} = 0, \quad \frac{\partial v}{\partial \mathbf{n}}\Big|_{\partial\Omega} = 0\Big\}. \tag{2.2b}$$

We introduce the space of Bogner-Fox-Schmit rectangles, $V_3^{(1)}$. On each rectangle, the Q_3 polynomials are determined by 16 nodal degrees of freedom, depicted in the first diagram in Fig. 1. To be precise, the Bogner-Fox-Schmit rectangle is defined in [10] by the triple $(\hat{Q},\Sigma,Q_3)$:

$$\begin{aligned} \hat{Q} &= (0,1)\times(0,1),\\ \Sigma &= \big\{v(a_i), v_x(a_i), v_y(a_i), v_{xy}(a_i), \quad i=1,2,3,4\big\}, \end{aligned}$$

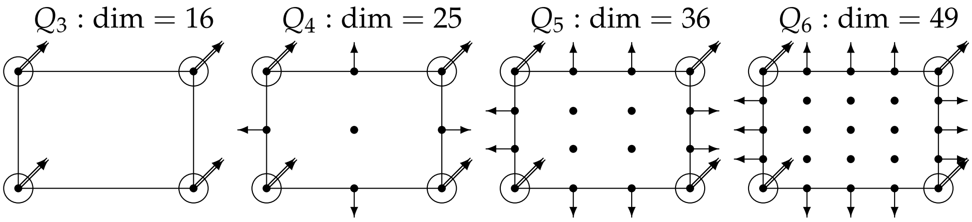

Figure 1: The family of Bogner-Fox-Schmit rectangles, cf. (2.6).

where a_i are the four vertices of $\hat{Q}$. Note that

$$\dim Q_3 = \dim \Sigma = 16.$$

Let $\hat{\phi}_l$ be the 16 nodal basis functions on $\hat{Q}$. Then

$$V_3^{(1)} = \text{span}\left\{ v_l(x,y) \in V_3 \middle| \, v_l\big(F|_{\Omega_{ij}}(\hat{x},\hat{y})\big) = \hat{\phi}_{l'}, \quad \forall \Omega_{ij} \in \Omega_h \right\},$$

where F is the affine reference mapping for the rectangle Ω_{ij}, and l' is the corresponding local index for the global index l. It is shown in [10], i.e.,

$$V_3^{(1)} \subset V_3.$$

It will be shown that

$$V_3^{(1)} = V_3.$$

To define one type of extension of the Bogner-Fox-Schmit Q_3 element, we study the element as a tensor product of the cubic Hermit splines. Let the 4 cubic spline basis functions on $[0,1]$ be

$$\hat{\phi}_0(x) = x^3 - 2x^2 + x, \qquad \hat{\phi}_1(x) = 2x^3 - 3x^2 + 1, \tag{2.3a}$$
$$\hat{\phi}_2(x) = -2x^3 + 3x^2, \qquad \hat{\phi}_3(x) = x^3 - x^2. \tag{2.3b}$$

It can be shown (cf. [20]) that on each rectangle Ω_{ij}

$$\begin{aligned} v(x,y) = \sum_{m,l=0}^{1} & v(x_{i+m}, y_{j+l})\phi_{i,m+1}(x)\phi_{j,l+1}(y) \\ & + hv_x(x_{i+m}, y_{j+l})\phi_{i,3m}(x)\phi_{j,l+1}(y) \\ & + hu_y(x_{i+m}, y_{j+l})\phi_{i,m+1}(x)\phi_{j,3l}(y) \\ & + h^2 u_{xy}(x_{i+m}, y_{j+l})\phi_{i,3m}(x)\phi_{j,3l}(y), \qquad \forall v \in V_3^{(1)}, \end{aligned}$$

where the basis functions (after the reference mapping) are

$$\phi_{i,l}(x) = \hat{\phi}_l\Big(\frac{x - x_i}{h}\Big), \qquad \phi_{j,l}(y) = \hat{\phi}_l\Big(\frac{y - y_j}{h}\Big).$$

Here (x_i, y_j) is the lower-left corner of rectangle Ω_{ij}. Similarly, let $\{\hat{\phi}_i(x)\}$ be the $(k+1)$ basis functions for the C_1-P_k splines on $[0,1]$, i.e.,

$$\hat{\phi}_0'(0) = 1, \quad \hat{\phi}_l\Big(\frac{j-1}{k-2}\Big) = \delta_{lj}, \quad \hat{\phi}_k'(1) = 1, \quad j, l = 1, 2, \cdots, k-1, \tag{2.4}$$

and $\hat{\phi}_l$ is zero when evaluated by the other k functionals. For example, the basis functions for k=3 and k=4 are listed in (2.3) and (4.3), respectively. The first family of C_1-Q_k finite elements are defined by

$$V_k^{(1)} = \Big\{ v(x,y) \in C(\Omega) \Big|\, v|_{\Omega_{mn}} = \sum_{0\le i,j\le k} v_{ij}\phi_i(x)\phi_j(y), \quad \forall \Omega_{mn} \in \Omega_h \Big\}, \tag{2.5}$$

where

$$v_{ij} = \begin{cases} v\big(x_m + \frac{i-1}{k-2}h, y_n + \frac{j-1}{k-2}h\big), & 0 < i, j < k, \\ v_x\big(x_m + \frac{i}{k}h, y_n + \frac{j-1}{k-2}h\big), & i = 0, k, \ \ 0 < j < k, \\ v_y\big(x_m + \frac{i-1}{k-2}h, y_n + \frac{j}{k}h\big), & j = 0, k, \ \ 0 < i < k, \\ v_{xy}\big(x_m + \frac{i}{k}h, y_n + \frac{j}{k}h\big), & i, j = 0, k, \end{cases}$$

$$\phi_i(x) = \begin{cases} \hat{\phi}_i\big(\frac{x-x_m}{h}\big), & 0 < i < k, \\ h\hat{\phi}_i\big(\frac{x-x_m}{h}\big), & i = 0, k, \end{cases}$$

$$\phi_j(y) = \begin{cases} \hat{\phi}_j\big(\frac{y-y_n}{h}\big), & 0 < j < k, \\ h\hat{\phi}_j\big(\frac{y-y_n}{h}\big), & j = 0, k. \end{cases}$$

At this moment, the relation between V_k and $V_k^{(1)}$ is not clear that either $V_k \not\subset V_k^{(1)}$ or $V_k \not\supset V_k^{(1)}$ may happen, as we do not know if $V_k^{(1)} \subset C_1$. To study this inclusion, we find an equivalent definition of (2.5).

Theorem 2.1. *The finite element space* $V_k^{(1)}$ *of* (2.5) *is equivalently defined by the finite element triple:*

$$\Big(\hat{Q},\ \Sigma^{(1)},\ Q_k\Big), \tag{2.6}$$

where $\Sigma^{(1)}$ *is defined by (see Fig. 1)*

$$\begin{aligned} \Sigma^{(1)} = \Big\{ & v\Big(\frac{i}{k-2}, \frac{j}{k-2}\Big), \quad 0 \le i, j \le k-2, \\ & v_y\Big(\frac{i}{k-2}, j\Big), \quad 0 \le i \le k-2 \text{ and } j = 0, 1, \\ & v_x\Big(j, \frac{i}{k-2}\Big), \quad 0 \le i \le k-2 \text{ and } j = 0, 1, \\ & v_{xy}(i, j), \quad 0 \le i, j \le 1 \Big\}, \end{aligned}$$

and the reference element $\hat{Q}$ *is the unit square.*

Proof. It is straightforward to verify the tensor product basis defined in (2.4) and (2.5) is the dual basis for the space of functionals $\Sigma^{(1)}$ on $\hat{Q}$. □

Remark 2.1. The definition of finite element space here by the triple $(\hat{Q}, \Sigma^{(1)}, Q_k)$ needs some additional arguments, as $\Sigma^{(1)}$ is defined on a subset of $H_2(\Omega)$ because the mixed second derivatives at vertices are used. We require that the nodal value interpolation operator associated with $\Sigma^{(1)}$ preserve functions in $V_k^{(1)}$. We may define the interpolation operator as a boundary averaging operator similar to that defined in Scott-Zhang [31], which is identical to the nodal interpolation operator when restricted to Q_k. We refer to Ciarlet [10] for more discussions on how to define C_1 finite element spaces by high order nodal derivatives.

Theorem 2.2. *The functional set $\Sigma^{(1)}$ defined in* (2.6) *is uni-solvent for the finite element triple $(\hat{Q}, \Sigma^{(1)}, Q_k)$, where $\hat{Q}$ is the reference square.*

Proof. Let

$$q(x,y) \in Q_k \quad \text{and} \quad f_l(q) = 0,$$

for all $(k+1)^2$ functionals $f_l \in \Sigma^{(1)}$. Let $L_j(x)=0$ be a vertical line passing through some of the $(k+1)^2$ interpolation points, i.e.,

$$L_j(x) = x - \frac{j}{k-2}, \qquad j = 0, 1, \cdots, k-2.$$

When restricted on

$$L_j(x) = 0 \quad \text{or} \quad L_j(y) = 0,$$

$q(x,y)$ is a degree k polynomial in y or x, respectively. As $q(x,y)$ is zero at $(k-1)$ points on the line segment $[0,1]\times[0,0]$ and $q_x(x,y)$ is zero at the two end points, $q(x,y)$ is identically zero on the line segment, i.e.,

$$q(x,y) = L_0(y) q_1(x,y).$$

Next, because $q_y(x,y)$ is zero at $(k-1)$ points on the line segment $[0,1]\times[0,0]$ and $q_{xy}(x,y)$ is zero at the two end points, we can factor out another factor

$$q(x,y) = L_0^2(y) q_2(x,y).$$

By symmetry,

$$q(x,y) = L_0^2(x) L_{k-2}^2(x) L_0^2(y) L_{k-2}^2(y) q_3(x,y), \qquad q_3 \in Q_{k-4}.$$

For $1 \le j \le k-3$, $L_j(y)=0$ is a line passing through $(k-3)$ internal interpolation points (see Fig. 1). Since q has $(k-3)$ internal zeros, two boundary zeros, and two tangential derivative (normal to $x=0,1$) zeros at the two ends, on $L_j(y)=0$, we conclude that we can factor out $L_j(y)$ from q, i.e.,

$$q(x,y) = L_0^2(x) L_{k-2}^2(x) L_j(y) L_0^2(y) L_{k-2}^2(y) q_4(x,y).$$

By symmetry,

$$q(x,y) = L_0(x)L_{k-2}(x)L_0(y)L_{k-2}(y)\prod_{i,j=0}^{k-2} L_i(x)L_j(y)q_5(x,y),$$

thus, $q(x,y)$ is a product of a Q_{k+1} polynomial with another polynomial $q_5(x,y)$. This leads the conclusion $q_5(x,y)$ is a polynomial of degree negative one. So

$$q(x,y) \equiv 0,$$

the proof is completed. $\square$

One of our goals is to find out the structure, or a basis for V_k. Before we show

$$V_k = V_k^{(1)},$$

we would try another extension of the Bogner-Fox-Schmit Q_3 element, where we can get more global degrees of freedom. But the finite element spaces are no longer C_1. Again, let Ω_h be defined in (2.1). We count the dimension $V_k^{(1)}$ by the definition $\Sigma^{(1)}$ in (2.6)

$$\begin{aligned}\dim V_k^{(1)} =& 4V + 2(k-3)E + (k-3)^2K\\ =& 4(N+1)^2 + 4(k-3)N(N+1) + (k-3)^2N^2\\ =& (k-1)^2N^2 + 4(k-1)N + 4\\ =& \big((k-1)N+2\big)^2,\end{aligned} \tag{2.7}$$

where V, E and K denote the number of vertices, of edges, and of squares, respectively, in Ω_h (of $N \times N$ rectangles). Noting that each nodal degree of freedom at a vertex is shared by 4 elements, while that inside an edge is shared by 2. One would expect more total degrees of freedom, if moving some functionals at vertex to interior-edge points. We may replace the mixed 2nd-order derivative at each vertex by two normal derivatives at internal points on edges. To ensure the C_1 continuity on each edge, we would have two additional normal derivatives specified inside each edge, based on $\Sigma^{(1)}$. This would lead to

$$\Sigma_3^{(2)} = \Sigma' \bigcup \Big\{ v_y\Big(\frac{i}{3}, j\Big) \ \&\ v_x\Big(j, \frac{i}{3}\Big), \quad 1 \le i \le 2 \text{ and } j = 0,1 \Big\}, \tag{2.8a}$$

$$\begin{aligned}\Sigma_4^{(2)} = \Sigma' \bigcup \Big\{ & v_y\Big(\frac{i}{4}, j\Big) \ \&\ v_x\Big(j, \frac{i}{4}\Big), \quad 1 \le i \le 3 \text{ and } j = 0,1;\\ & v\Big(\frac{i}{2}, j\Big) \ \&\ v\Big(j, \frac{i}{2}\Big), \quad 1 \le i \le 1 \text{ and } j = 0,1 \Big\},\end{aligned} \tag{2.8b}$$

$$\begin{aligned}\Sigma_5^{(2)} = \Sigma' \bigcup \Big\{ & v_y\Big(\frac{i}{5}, j\Big) \ \&\ v_x\Big(j, \frac{i}{5}\Big), \quad 1 \le i \le 4 \text{ and } j = 0,1;\\ & v\Big(\frac{i}{3}, j\Big) \ \&\ v\Big(j, \frac{i}{3}\Big), \quad 1 \le i \le 2 \text{ and } j = 0,1 \Big\},\end{aligned} \tag{2.8c}$$

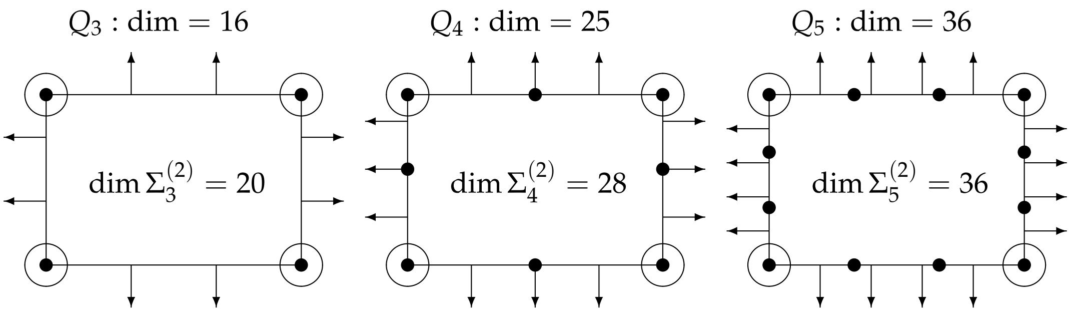

Figure 2: Non-unisolvent sets $\Sigma_k^{(2)}$, cf. (2.8a)–(2.8c).

where

$$\Sigma' = \Big\{ v(i,j),\ v_y(i,j) \& \ v_x(i,j), \quad i = 0,1 \text{ and } j = 0,1 \Big\}.$$

This cannot be done for Q_3 and Q_4 because their dimensions are less than the number of functionals in $\Sigma_3^{(2)}$ and $\Sigma_4^{(2)}$, respectively, as shown in the first two diagrams in Fig. 2. Can we define $\Sigma_5^{(2)}$ in (2.8c) for Q_5 as depicted in Fig. 2? Can we define such a $\Sigma^{(2)}$ for Q_k for all $k \geq 5$? The answer is no. First, such a $\Sigma^{(2)}$ would not define a global C_1 space. Second, such a $\Sigma^{(2)}$ does not even resolve a Q_5 polynomial, as we have too many constraints on the boundary.

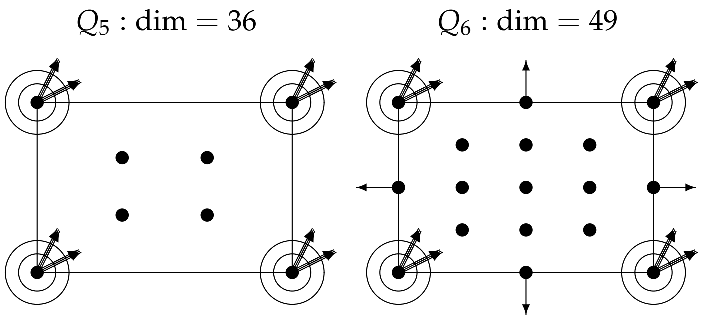

Figure 3: The second family of C_1-Q_k elements, defined in (2.9).

Let us try the opposite direction, moving some nodal freedoms from interior-edge points to the vertices. For $k \geq 5$, this can be done. Let $\Sigma_k^{(3)}$ be shown in Fig. 3, i.e.,

$$\begin{aligned}
\Sigma^{(3)} = \Big\{ & v\Big(\frac{i}{k-4}, j\Big),\ v_y\Big(\frac{i}{k-4}, j\Big),\ v_x\Big(j, \frac{i}{k-4}\Big), \quad 0 \leq i \leq (k-4),\ j = 0,1; \\
& v\Big(i, \frac{j}{k-4}\Big), \quad 1 \leq j \leq (k-5),\ i = 0,1; \\
& v_{xx}(i,j),\ v_{yy}(i,j),\ v_{xy}(i,j), \quad 0 \leq i,j \leq 1; \\
& v_{xxy},\ v_{xyy}(i,j), \quad 0 \leq i,j \leq 1; \\
& v\Big(\frac{i}{k-2}, \frac{j}{k-2}\Big), \quad 1 \leq i,j \leq (k-3) \Big\}.
\end{aligned} \tag{2.9}$$

Then, the finite element space defined by $(\hat{Q}, \Sigma^{(3)}, Q_k)$ on the grid Ω_h is

$$V_k^{(3)} = \text{span}\left\{ v_l(x,y) \in C(\Omega) \,\middle|\, v_l(F^{-1}(x,y))|_{\Omega_{mn}} \in \text{span}\,(\Sigma^{(3)'}),\ \forall \Omega_{mn} \in \Omega_h \right\}. \tag{2.10}$$

Here $V_k^{(3)}$ is the span of global basis functions which are the mapped dual basis functions of $\Sigma^{(3)}$ on each rectangle Ω_{mn}.

Theorem 2.3. *The functional set $\Sigma^{(3)}$ defined in* (2.10) *is uni-solvent for the finite element triple $(\hat{Q}, \Sigma^{(3)}, Q_k)$, where $\hat{Q}$ is the reference square.*

Proof. The proof is nearly identical to that for Theorem 2.2. Let

$$q(x,y) \in Q_k \quad \text{and} \quad f_l(q) = 0,$$

for all $(k+1)^2$ functionals of $\Sigma^{(3)}$. As in Theorem 2.2, we have

$$q(x,y) = L_0^2(x) L_{k-2}^2(x) L_0^2(y) L_{k-2}^2(y) q_3(x,y), \quad q_3 \in Q_{k-4}.$$

For $1 \leq j \leq (k-3)$, $L_j(y)=0$ is a horizontal line passing through $(k-3)$ internal interpolation points (see Fig. 3). Different from Theorem 2.2, there is no nodal freedom at the two end points of line segment $L_j(y)=0$. But we show above q has zero values and zero normal derivatives at the two ends, i.e., when $x=0,1$. We conclude that we can still factor out $L_j(y)$ from q. Therefore,

$$q(x,y) = L_0(x) L_{k-2}(x) L_0(y) L_{k-2}(y) \prod_{i,j=0}^{k-2} L_i(x) L_j(y) q_5(x,y).$$

As $q_5(x,y)$ is a polynomial of degree negative one,

$$q(x,y) \equiv 0,$$

so the proof is completed. ☐

Similar to (2.7), we count the dimension $V_k^{(3)}$ as follows:

$$\begin{aligned} \dim V_k^{(3)} &= 8V + 2(k-5)E + (k-3)^2 K \\ &= 8(N+1)^2 + 4(k-5)N(N+1) + (k-3)^2 N^2 \\ &= \big((k-1)N+2\big)^2 - 4(N^2-1). \end{aligned} \tag{2.11}$$

Compared with $\dim V_k^{(1)}$, the dimension of the new family of element is reduced by $4(N^2-1)$. Strang gave a conjecture on the dimension of piecewise C_1 polynomials V_h, based on the inter-element constraint, cf. [5,23,33,34], that

$$\dim V_h = K \cdot \dim V_K - E_0 \cdot C_e + V_0 \cdot C_v + \sigma, \tag{2.12}$$

where V_K is the space of V_h restricted on one element, K the number of elements, E_0 the number of internal edges, V_0 the number of internal vertices, C_e the number of constraints for continuity on each edge, C_v the number of freedoms at each vertex, and σ is the number of singular vertices. A vertex is singular if all edges meeting at the vertex fall into two cross lines (cf. Fig. 6). Though Strang made the conjecture for triangular grids, we apply it to our C_1-Q_k space V_k on the $(n \times n)$ rectangular grid Ω_h.

$$\begin{aligned}\dim V_h =&K(k+1)^2 - E_0(2k+2) + V_0(3) + \sigma \\ =&N^2(k+1)^2 - 2N(N-1)(2k+2) + (N-1)^2(3) + (N-1)^2 \\ =&N^2(k-1)^2 + N(4k-4) + 4 \\ =&\big((k-1)N+2\big)^2. \end{aligned} \tag{2.13}$$

Here

$$C_e = 2k+2,$$

to match the $(k+1)$ function values and $(k+1)$ normal derivatives on two sides of an edge of a piecewise Q_k function, and C_v=3 for the function value and two first derivatives to be the same at a vertex for a piecewise Q_k function. We note that the conjectured $\dim V_k$ is equal to $\dim V_k^{(1)}$, see (2.7). If the Strang's conjecture is correct, we would immediately conclude that

$$V_k^{(1)} = V_k \quad (\text{assuming } V_k^{(1)} \text{ is } C_1).$$

Nevertheless, the conditions for the Strang's conjecture are not yet fully discovered, cf. [23]. Therefore, we have to prove $V_k^{(1)}$=V_k directly. By this proof, we verify the Strang's conjecture on the rectangular grids.

Theorem 2.4. *Let V_k, $V_k^{(1)}$ and $V_k^{(3)}$ be defined in* (2.2a), (2.5) *and* (2.10), *respectively. It holds that*

$$V_k^{(1)} = V_k, \qquad V_k^{(3)} \underset{\neq}{\subset} V_k \subset C_1(\Omega).$$

Proof. We prove $V_k^{(1)} \subset V_k$ first. Since each function in $V_k^{(1)}$ is a piecewise Q_k polynomial, we need to show then $V_k^{(1)} \subset C_1(\Omega)$. For a function $q \in V_k^{(1)}$, we can write it as a linear combination of monomials on each element. In particular, for the four elements of Ω_{mn} meeting at the vertex (x_m, y_n), we denote

$$q|_{\Omega_{m+t,n+s}} = \sum_{i,j=0}^{k} q_{ij}^{(l)} (x-x_m)^i (y-y_n)^j, \qquad t,s = -1,0, \tag{2.14}$$

where

$$l = 2(1+t) + (1+s).$$

x^4y^4	x^3y^4	x^2y^4	xy^4	y^4	y^4	xy^4	x^2y^4	x^3y^4	x^4y^4
x^4y^3	x^3y^3	x^2y^3	xy^3	y^3	y^3	xy^3	x^2y^3	x^3y^3	x^4y^3
x^4y^2	x^3y^2	x^2y^2	xy^2	y^2	y^2	xy^2	x^2y^2	x^3y^2	x^4y^2
x^4y	x^3y	x^2y	xy	y	y	xy	x^2y	x^3y	x^4y
x^4	x^3	x^2	x	1	1	x	x^2	x^3	x^4
x^4	x^3	x^2	x	1	1	x	x^2	x^3	x^4
x^4y	x^3y	x^2y	xy	y	y	xy	x^2y	x^3y	x^4y
x^4y^2	x^3y^2	x^2y^2	xy^2	y^2	y^2	xy^2	x^2y^2	x^3y^2	x^4y^2
x^4y^3	x^3y^3	x^2y^3	xy^3	y^3	y^3	xy^3	x^2y^3	x^3y^3	x^4y^3
x^4y^4	x^3y^4	x^2y^4	xy^4	y^4	y^4	xy^4	x^2y^4	x^3y^4	x^4y^4

$q^{(1)}_{44}$	$q^{(1)}_{34}$	$q^{(1)}_{24}$	$q^{(1)}_{14}$	$q^{(1)}_{04}$	$q^{(3)}_{04}$	$q^{(3)}_{14}$	$q^{(3)}_{24}$	$q^{(3)}_{34}$	$q^{(3)}_{44}$
$q^{(1)}_{43}$	$q^{(1)}_{33}$	$q^{(1)}_{23}$	$q^{(1)}_{13}$	$q^{(1)}_{03}$	$q^{(3)}_{03}$	$q^{(3)}_{13}$	$q^{(3)}_{23}$	$q^{(3)}_{33}$	$q^{(3)}_{43}$
$q^{(1)}_{42}$	$q^{(1)}_{32}$	$q^{(1)}_{22}$	$q^{(1)}_{12}$	$q^{(1)}_{02}$	$q^{(3)}_{02}$	$q^{(3)}_{12}$	$q^{(3)}_{22}$	$q^{(3)}_{32}$	$q^{(3)}_{42}$
$q^{(1)}_{41}$	$q^{(1)}_{31}$	$q^{(1)}_{21}$	$q^{(1)}_{11}$	$q^{(1)}_{01}$	$q^{(3)}_{01}$	$q^{(3)}_{11}$	$q^{(3)}_{21}$	$q^{(3)}_{31}$	$q^{(3)}_{41}$
$q^{(1)}_{40}$	$q^{(1)}_{30}$	$q^{(1)}_{20}$	$q^{(1)}_{10}$	$q^{(1)}_{00}$	$q^{(3)}_{00}$	$q^{(3)}_{10}$	$q^{(3)}_{20}$	$q^{(3)}_{30}$	$q^{(3)}_{40}$
$q^{(0)}_{40}$	$q^{(0)}_{30}$	$q^{(0)}_{20}$	$q^{(0)}_{10}$	$q^{(0)}_{00}$	$q^{(2)}_{00}$	$q^{(2)}_{10}$	$q^{(2)}_{20}$	$q^{(2)}_{30}$	$q^{(2)}_{40}$
$q^{(0)}_{41}$	$q^{(0)}_{31}$	$q^{(0)}_{21}$	$q^{(0)}_{11}$	$q^{(0)}_{01}$	$q^{(2)}_{01}$	$q^{(2)}_{11}$	$q^{(2)}_{21}$	$q^{(2)}_{31}$	$q^{(2)}_{41}$
$q^{(0)}_{42}$	$q^{(0)}_{32}$	$q^{(0)}_{22}$	$q^{(0)}_{12}$	$q^{(0)}_{02}$	$q^{(2)}_{02}$	$q^{(2)}_{12}$	$q^{(2)}_{22}$	$q^{(2)}_{32}$	$q^{(2)}_{42}$
$q^{(0)}_{43}$	$q^{(0)}_{33}$	$q^{(0)}_{23}$	$q^{(0)}_{13}$	$q^{(0)}_{03}$	$q^{(2)}_{03}$	$q^{(2)}_{13}$	$q^{(2)}_{23}$	$q^{(2)}_{33}$	$q^{(2)}_{43}$
$q^{(0)}_{44}$	$q^{(0)}_{34}$	$q^{(0)}_{24}$	$q^{(0)}_{14}$	$q^{(0)}_{04}$	$q^{(2)}_{04}$	$q^{(2)}_{14}$	$q^{(2)}_{24}$	$q^{(2)}_{34}$	$q^{(2)}_{44}$

Figure 4: The monomial ordering at $(0,0)$ and the coefficients, cf. (2.14).

Here l=0,1,2,3 (cf. Fig. 4.) We depict the terms in Fig. 4 for k=4, shifting the vertex (x_m, y_n) to the origin $(0,0)$.

Let

$$y = y_n,$$

by the definition of $\Sigma^{(1)}$, q is uniquely defined on (both sides of) the line segment, and that (see Fig. 4)

$$q^{(0)}_{i0} = q^{(1)}_{i0}, \quad q^{(2)}_{i0} = q^{(3)}_{i0}, \quad i = 0, 1, \cdots, k.$$

Next, as q_y is uniquely determined by the functionals of $\Sigma^{(1)}$, it follows

$$q^{(0)}_{i1} = q^{(1)}_{i1}, \quad q^{(2)}_{i1} = q^{(3)}_{i1}, \quad i = 0, 1, \cdots, k.$$

On the other direction, as q and q_x are determined by the nodal freedoms on the line x=x_m, we have also

$$q^{(0)}_{ij} = q^{(1)}_{ij}, \quad q^{(2)}_{ij} = q^{(3)}_{ij}, \quad i = 0, 1 \quad \text{and} \quad j = 0, 1, \cdots, k.$$

In particular, the four coefficients at the center (see Fig. 4) are the same

$$q^{(0)}_{ij} = q^{(l)}_{ij}, \quad l = 1, 2, 3 \quad \text{and} \quad i, j = 0, 1. \tag{2.15}$$

Hence q is C_1 on the four rectangles

$$q \in C_1\Big(\bigcup_{t,s=-1}^{0} \Omega_{m+t,n+s} \Big).$$

As (x_m, y_n) is a generic vertex of Ω_h, we conclude that

$$q \in C_1(\Omega).$$

Next we prove $V_k^{(1)} \supset V_k$. Let $q \in V_k$. We expand q again as a combination of monomials on each rectangle Ω_{mn}. Consider q on the four rectangles $\Omega_{m+t,n+s}$ again. Since $q \in C_1$, the two rows of coefficients of q above the horizontal line (see Fig. 4) and those below the horizontal line would match the nodal freedoms defined by $\Sigma^{(1)}$. Similarly for the two columns of coefficients of q on the two sides of the vertical grid line. Thus, at the intersection point, we have

$$\begin{aligned} q_{00}^{(l)} &= q(x_m, y_n), \qquad & q_{10}^{(l)} &= q_x(x_m, y_n), \\ q_{01}^{(l)} &= q_y(x_m, y_n), \qquad & q_{11}^{(l)} &= q_{xy}(x_m, y_n), \end{aligned}$$

for $l=0,1,2,3$. Therefore, we have

$$I_k^{(1)} q = q,$$

where $I_k^{(1)}$ is the global nodal interpolation operator associated with $\Sigma^{(1)}$ and Ω_h (see [10] for the standard definition). Hence

$$q = I_k^{(1)} q \in V_k^{(1)}.$$

The proof for $V_k^{(3)} \subset V_k$ is similar. To show $V_k^{(3)} \not\supset V_k$, we can simply use the dimension counts (2.7) and (2.11) to get

$$\dim V_k^{(3)} < \dim V_k^{(1)} = \dim V_k,$$

or we may prove this directly. Let

$$q \in V_k = V_k^{(1)},$$

be such that (cf. Fig. 4 and (2.15)) the four values $q_{x^2 y}^{(l)}(x_m, y_n)$ on the four rectangles around a vertex are not same. This property must hold for all $V_k^{(3)}$ functions. Thus

$$q \notin V_k^{(3)},$$

so the theorem is proved. $\square$

The Strang's conjecture is not yet proved in general. But it is true in our special case, the Q_k element on a square grid.

Corollary 2.1. *The Strang's conjecture* (2.12) *is valid for rectangular grids on a square.*

Proof. By Theorem 2.4,

$$V_k = V_k^{(1)}.$$

The dimension of $V_k^{(1)}$ is calculated in (2.7), which matches the dimension of C_1 polynomial spaces predicted by the Strang's conjecture in (2.13). $\square$

3 C_1-Q_k finite elements on 3D rectangular grids

In this section, we extend the 2D Bogner-Fox-Schmit rectangles to 3D C_1-Q_3 cuboids, and further to a whole family of C_1-Q_k finite elements.

When extending the Bogner-Fox-Schmit element to 2D C_1-Q_k elements, we gave two equivalent definitions, (2.5) and (2.6), by the tensor products of 1D splines $\{\hat{\phi}_i\}$ and by the nodal value functionals $\Sigma^{(1)}$. We do the same for the 3D extension.

In this section, we denote the unit cube, the 3D reference element, again by $\hat{Q}$, i.e.,

$$\hat{Q} = (0,1)^3.$$

We define the finite element triple $(\hat{Q}, \Sigma^{(4)}, Q_k)$, where Q_k is the space of 3D polynomials of separate degree k or less, and

$$\begin{aligned}
\Sigma^{(4)} = \Big\{ & v\Big(\frac{i}{k-2}, \frac{j}{k-2}, \frac{l}{k-2}\Big), \quad 0 \le i,j,l \le (k-2); \\
& v_x\Big(i, \frac{j}{k-2}, \frac{l}{k-2}\Big), \quad 0 \le j,l \le (k-2) \quad \text{and} \quad i = 0,1; \\
& v_y\Big(\frac{i}{k-2}, j, \frac{l}{k-2}\Big), \quad 0 \le i,l \le (k-2) \quad \text{and} \quad j = 0,1; \\
& v_z\Big(\frac{i}{k-2}, \frac{j}{k-2}, l\Big), \quad 0 \le i,j \le (k-2) \quad \text{and} \quad l = 0,1; \\
& v_{xy}\Big(i, j, \frac{l}{k-2}\Big), \quad 0 \le i,j \le 1 \quad \text{and} \quad 0 \le l \le (k-2); \\
& v_{xz}\Big(i, \frac{j}{k-2}, l\Big), \quad 0 \le i,l \le 1 \quad \text{and} \quad 0 \le j \le (k-2); \\
& v_{yz}\Big(\frac{i}{k-2}, j, l\Big), \quad 0 \le j,l \le 1 \quad \text{and} \quad 0 \le i \le (k-2); \\
& v_{xyz}(i,j,l), \quad 0 \le i,j,l \le 1 \Big\}.
\end{aligned} \tag{3.1}$$

We plot the nodal freedoms of $\Sigma^{(4)}$ for k=3 in Fig. 5. We note that we start to have normal derivative at interior points of face rectangles when k>3.

Similar to the proof for $\Sigma^{(1)}$, we can show $\Sigma^{(4)}$ is uni-solvent. Then we can find the dual basis of $\Sigma^{(4)}$ and obtain the global nodal basis of piecewise Q_k functions via

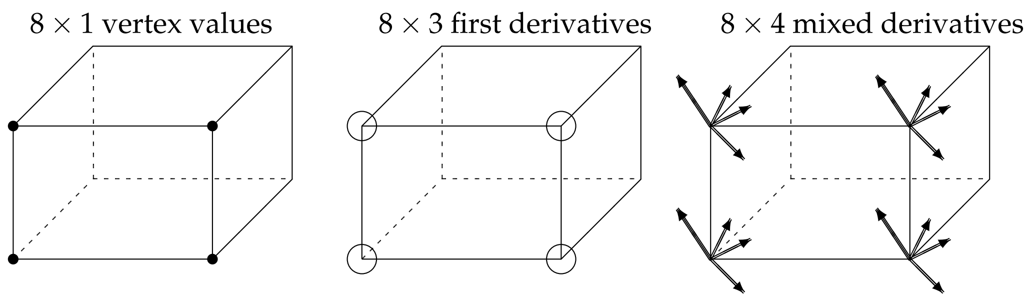

Figure 5: The C_1-Q_3 cuboid defined in (3.3) (shown only the front face nodal freedoms).

reference mappings. It is then standard to define the finite element space $V_k^{(4)}$ by the span of all nodal basis functions:

$$V_k^{(4)} = \text{span}\Big\{v_l(x,y,z)\Big|\ v_l \circ F^{-1}\big|_{\Omega_{mno}} \in \text{Span}\big(\Sigma^{(4)'}\big),\quad \forall\Omega_{mno} \in \Omega_h\Big\}, \tag{3.2}$$

where Ω_h is defined in (2.1). Next, we give an equivalent definition of $V_k^{(4)}$ by the tensor products of 1D splines. Let $\{\hat{\phi}_i\}$ be defined in (2.4), the splines on $[0,1]$,

$$V_k^{(4)} = \Big\{v\Big|\ v|_{\Omega_{mno}} = \sum_{0\le i,j,l\le k} v_{ijl}\phi_i(x)\phi_j(y)\phi_l(z),\quad \forall\Omega_{mno} \in \Omega_h\Big\}, \tag{3.3}$$

where

$$\phi_i(x) = \begin{cases} \hat{\phi}_i\big(\frac{x-x_m}{h}\big), & 0<i<k, \\ h\hat{\phi}_i\big(\frac{x-x_m}{h}\big), & i=0,k, \end{cases}$$
$$\phi_j(y) = \begin{cases} \hat{\phi}_j\big(\frac{y-y_n}{h}\big), & 0<j<k, \\ h\hat{\phi}_j\big(\frac{y-y_n}{h}\big), & j=0,k, \end{cases}$$
$$\phi_l(z) = \begin{cases} \hat{\phi}_l\big(\frac{z-z_o}{h}\big), & 0<l<k, \\ h\hat{\phi}_l\big(\frac{z-z_o}{h}\big), & l=0,k. \end{cases}$$

We note that the tensor products of 1D splines in (3.2) are the (dual) nodal basis functions for the $\Sigma^{(4)}$ in (3.1).

Theorem 3.1. *Let V_k and $V_k^{(4)}$ be defined by* (2.2a) *and* (3.3), *respectively. Then,*

$$V_k = V_k^{(4)}.$$

That is, every C_1-Q_k function is a linear combination of nodal basis functions in (3.3).

Proof. The technique is the same as that used in Theorem 2.4. As each tensor product basis function is C_1, by the definition, $V_k^{(4)} \subset V_k$. We write a piecewise Q_k function q in V_k as a combination of monomial basis $\{x^iy^jz^l\}$ on each cube of Ω_h, similar to the 2D case shown in Fig. 4 and (2.15). The coefficients of q under such a basis are exactly the nodal values used in $\Sigma^{(4)}$. We note that to be C_1 on an interface square, the coefficients of $x^iy^jz^l$ on the two sides must be the same. This would conclude $V_k \subset V_k^{(4)}$. $\square$

Let $\Omega=(0,1)^3$ and Ω_h be a uniform rectangular grid of size $h=1/N$. In Ω_h, there are $(N+1)^3$ vertices, $3N(N+1)^2$ edges, $3N^2(N+1)$ rectangles, and N^3 cuboids. By counting the global freedoms of $V_k^{(4)}$ via (3.1), we get

$$\begin{aligned} \dim V_k^{(4)} =& 8(N+1)^3 + 4(k-3)3N(N+1)^2 + 2(k-3)^2 3N^2(N+1) + (k-3)^3N^3 \\ =& \big((k-1)N+2\big)^3. \end{aligned} \tag{3.4}$$

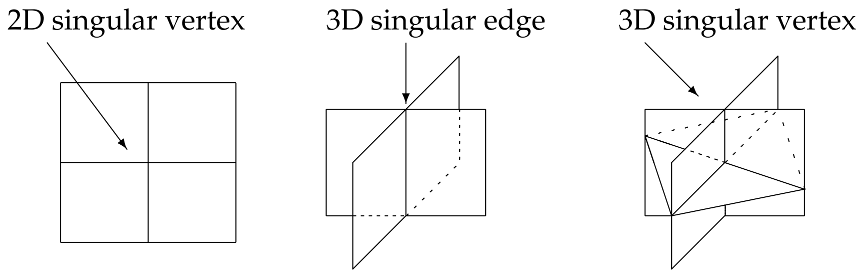

Figure 6: Singular vertices/edges (where some higher order derivatives are also continuous).

We give a generalization of the Strang's conjecture to 3D C_1 finite elements. Let V_h be a C_1 space of piecewise polynomials on a polygonal subdivision of Ω. Then the Strang's conjecture in 3D is

$$\dim V_h = K \cdot \dim V_K - F_0 \cdot C_f + E_0 \cdot C_e - V_0 \cdot C_v + \sigma_e \cdot f_e - 4\sigma_v, \tag{3.5}$$

where

$\dim V_K =$ the degree of freedom per element,
$K =$ the number of elements (polygons),
$F_0 =$ the number of inter-element (planar) faces,
$C_f =$ the number of C_1 constraints on each face,
$E_0 =$ the number of internal edges,
$C_e =$ the number of C_1 constraints on each edge,
$\sigma_e =$ the number of internal singular edges, where all inter-element faces fall into two cross planes (cf. Fig. 6),
$f_e =$ the degree of freedom on each edge,
$\sigma_v =$ the number of internal singular vertices, where all inter-element faces fall into three cross planes meeting at the vertex (cf. Fig. 6).

In the case of piecewise Q_k polynomials on every element, (3.5) becomes

$$\dim V_h = K(k+1)^3 - F_0 2(k+1)^2 + E_0 3(k+1) - V_0 4 + \sigma_e(k+1) - \sigma_v. \tag{3.6}$$

Further, if $\Omega=(0,1)^3$ is subdivided into N^3 uniform cubes, (3.5) is simplified to

$$\begin{aligned}\dim V_h =&(k+1)^3N^3 - 2(k+1)^2 3N^2(N-1) + 3(k+1)3N(N-1)^2\\ &- 4(N-1)^3 + (k+1)3N(N-1)^2 - 4(N-1)^3\\ =&\big((k-1)N+2\big)^3. \end{aligned}\tag{3.7}$$

Corollary 3.1. *The Strang's conjecture* (3.5) *is valid for 3D rectangular grids on a cube.*

Proof. By Theorem 3.1, $V_k^{(4)}=V_k(=V_h)$ in 3D. The dimension of $V_k^{(4)}$ is calculated in (3.4), which matches the dimension of C_1 polynomial spaces obtained by the generalized Strang's conjecture in (3.7). $\square$

We remark that the generalized conjecture (3.5) needs some refinements. For example, we need to revise it by including fractional-singular vertices, by which we mean, for example, the vertex $(1/2,1/2,1/2)$ of a uniform grid on domain $(0,1)^3 \setminus (1/2,1)^3$. In fact, the refinement or the conditions for the Strang's conjecture is far from complete, even in 2D, cf. [23].

4 Numerical tests

In this section, we perform some simple numerical tests on the 2D C_1-Q_k family of elements.

We solve the following biharmonic equation by the C_1-Q_k elements:

$$\Delta^2 u(x,y) = f(x,y), \quad \forall (x,y) \in \Omega, \tag{4.1a}$$

$$u|_{\partial\Omega} = 0, \quad \frac{\partial u}{\partial \mathbf{n}}\Big|_{\partial\Omega} = 0. \tag{4.1b}$$

The finite element problem in the variational form for (4.1) is: find $u_h \in V_{k,0}$ (see (2.2b)), such that

$$(\Delta u_h, \Delta v_h) = (f, v_h), \quad \forall v_h \in V_{k,0}. \tag{4.2}$$

The following theorem on the convergence is standard.

Theorem 4.1. *Let Ω_h be defined by* (2.1). *Let $V_{k,0}$ be defined by* (2.2b) *for $V_k=V_k^{(1)}$, or $V_k=V_k^{(3)}$, or $V_k=V_k^{(4)}$. Let u and u_h be solutions of* (4.1) *and* (4.2), *respectively. Then u_h approximates u at the optimal order*

$$|u-u_h|_{H_2(\Omega)} \le C h^{\min\{k+1,s\}-2} \|u\|_{H_s(\Omega)},$$

here s is the elliptic regularity order, cf. [6,19].

Proof. We have shown that the finite element spaces are C_1. Therefore the discrete solution is the Galerkin projection on the subspace. By Céa's Lemma (cf. [10]),

$$|u-u_h|_{H_2(\Omega)} \le C \inf_{v_h \in V_{k,0}} |u-v_h|_{H_2(\Omega)} \le C|u-I_h u|_{H_2(\Omega)},$$

where I_h is the nodal interpolation operator. In case u is not smooth enough that the nodal second or third derivatives are not well defined, we can let I_h be an averaging interpolation operator similar to the ones defined in [31] and [16]. Because $V_{k,0}$ is constructed with full Q_k locally and the interpolation operator I_h preserves Q_k polynomial locally, $I_h u$ approximates u at the optimal order, cf. [7,10]. $\square$

The domain for computation is simply the unit square $\Omega=(0,1)\times(0,1)$. We choose the exact solution (see Fig. 7 for its numerical approximation)

$$u(x,y) = \sin^6(\pi x)\sin^6(\pi y).$$

Then the right hand side function in the biharmonic equation (4.1) is

$$\begin{aligned} f =&\pi^4\big[360\sin^2(\pi x) - 1560\sin^4(\pi x) + 1296\sin^6(\pi x)\big]\sin^6(\pi y) \\ &+ 2\pi^4\big[30\sin^4(\pi x) - 36\sin^6(\pi x)\big]\big[30\sin^4(\pi y) - 36\sin^6(\pi y)\big] \\ &+ \pi^4\sin^6(\pi x)\big[360\sin^2(\pi y) - 1560\sin^4(\pi y) + 1296\sin^6(\pi y)\big]. \end{aligned}$$

The initial grid is the square, the domain itself. We refine the higher level grids by subdividing each square into 4. The grid size on the n-th grid is 2^{-n+1}. We first solve the problem by the C_1-Q_3 element, i.e., the Bogner-Fox-Schmit element. The nodal error on the 8×8 grid is plotted in the first diagram of Fig. 8.

In Table 1, we list the nodal errors in the maximum norm, and in the energy norm. The maximal-norm errors converge to 0 at the right order but the energy norm, i.e., the semi-H_2 norm, errors converge at two orders higher than the general theory predicts, see Theorem 4.1. Such a superconvergence property was studied in [20].

We test the new C_1-Q_4 element defined by (2.5). We note that, as shown in Section 2, the basis functions for C_1-Q_4 can be generated by the tensor product of the following 1D P_4 spline functions:

$$\hat{\phi}_0 = -2x^4 + 5x^3 - 4x^2 + x, \qquad \hat{\phi}_0'(0) = 1, \tag{4.3a}$$

$$\hat{\phi}_1 = -8x^4 + 18x^3 - 11x^2 + 1, \qquad \hat{\phi}_1(0) = 1, \tag{4.3b}$$

$$\hat{\phi}_2 = 16x^4 - 32x^3 + 16x^2, \qquad \hat{\phi}_2\Big(\frac{1}{2}\Big) = 1, \tag{4.3c}$$

$$\hat{\phi}_3 = -8x^4 + 14x^3 - 5x^2, \qquad \hat{\phi}_3(1) = 1, \tag{4.3d}$$

$$\hat{\phi}_4 = 2x^4 - 3x^3 + x^2, \qquad \hat{\phi}_4'(1) = 1. \tag{4.3e}$$

The new C_1-Q_4 element also performs better than that predicted by the theory, see Theorem 4.1. We listed the error in the energy norm, and in the maximum norm (for nodal errors), in Table 2. The energy-norm convergence seems to be one order higher than that of typical finite elements of degree 4 polynomials (cf. [10]). Here we should have a superconvergence too in function nodal values. This is known, summarized by

Table 1: The convergence of C_1-Q_3 (Bogner-Fox-Schmit) element.

Grid	# unknowns	$\lvert I_h u - u_h\rvert_{H_2}$	$\mathcal{O}(h^m)$	$\lvert u - u_h\rvert_{l_\infty}$	$\mathcal{O}(h^m)$
2×2	4	244.5235144		17.80019728	
4×4	36	17.3017418	3.82	0.59618802	4.89
8×8	196	0.2047198	6.40	0.00098388	9.24
16×16	900	0.0143049	3.83	0.00007040	3.80
32×32	3844	0.0009136	3.96	0.00000445	3.98

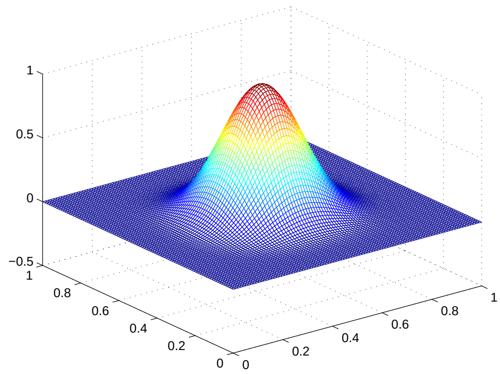

Figure 7: The solution of (4.1) by the C_1-Q_3 finite element.

Wahlbin for locally symmetric grids in [35]. When compared with the C_1-Q_3 element, as expected, the C_1-Q_4 solution can provide a better accuracy with less unknowns on coarse grids.

Finally, we list the numerical results for further higher order C_1-Q_k elements in Table 3. However, the computer accuracy in Matlab is not high enough for our imple-

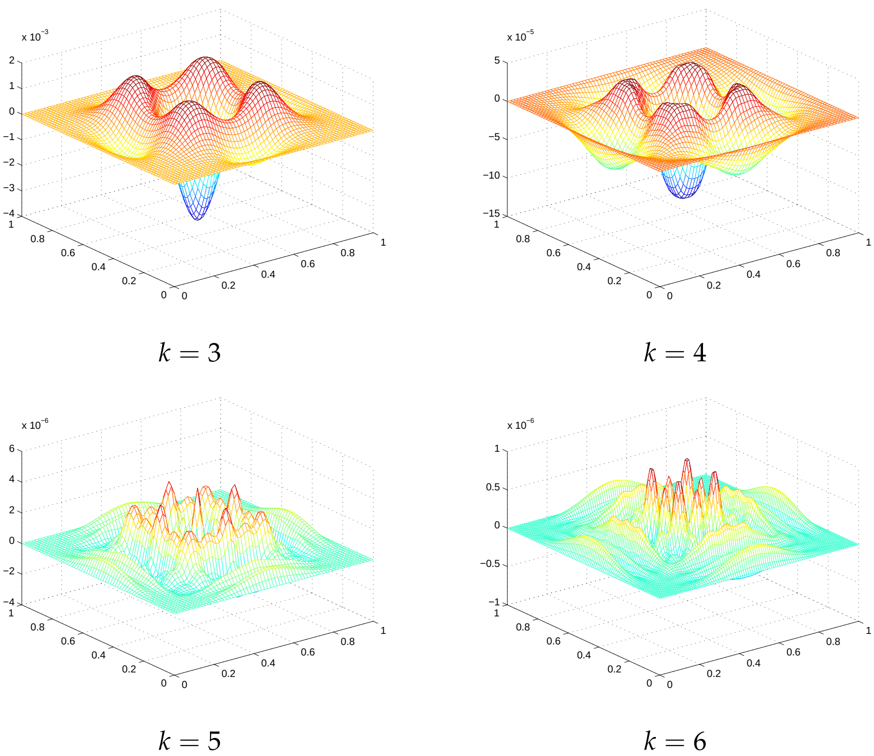

Figure 8: The nodal error of C_1-Q_k elements, for (4.1).

Table 2: The convergence of C_1-Q_4 (new) element.

Grid	# unknowns	$\|I_h u - u_h\|_{H_2}$	$\mathcal{O}(h^m)$	$\|u - u_h\|_{l_\infty}$	$\mathcal{O}(h^m)$
1×1	1	297.28721768		8.8678654571	
2×2	24	33.62082218	3.14	2.4776861911	3.32
4×4	116	1.65666367	4.34	0.0543605016	5.51
8×8	516	0.01038290	7.31	0.0000501649	10.08
16×16	2180	0.00052894	4.29	0.0000007102	6.14
32×32	8964	0.00003212	4.04	0.0000000121	5.86

mentation. The round off error dominates the truncation error on some fine grids. The convergence rates are of the optimal orders, shown at lower level grids.

Table 3: The convergence of C_1-Q_k elements, $5 \leq k \leq 7$.

Grid	degree	$\|I_h u - u_h\|_{H_2}$	$\mathcal{O}(h^m)$	$\|\|I_h u - u_h\|\|_{L^2}$	$\mathcal{O}(h^m)$
1×1	5	84.49527		2.349618341	
2×2	5	9.11393	3.21	0.237401792	3.30
4×4	5	0.07325	6.95	0.001359648	7.44
8×8	5	0.00228	5.00	0.000000835	10.66
16×16	5	0.00012	4.23	0.000000013	5.91
1×1	6	49.90785		1.317214962	
2×2	6	2.02852	4.62	0.051355068	4.68
4×4	6	0.02660	6.25	0.000425660	6.91
8×8	6	0.00063	5.38	0.000000145	11.51
16×16	6	0.00001	5.00	0.000000033	2.10
1×1	7	9.10576		0.087387136	
2×2	7	0.52529	4.11	0.010946550	2.99
4×4	7	0.00684	6.26	0.000029777	8.52
8×8	7	0.00011	5.87	0.000000137	7.75
16×16	7	0.00007	0.55	0.000002220	−−

References

[1] R. AITBAYEV, *Multilevel preconditioners for a quadrature Galerkin solution of a biharmonic problem*, Numer. Method. Partial. Differ. Eqs., 22 (2006), pp. 847–866.

[2] J. H. ARGYRIS, I. FRIED AND D. W. SCHARPF, *The TUBA family of plate elements for the matrix displacement method,* Aero. J. Roy. Aero. Soc., 72 (1968), pp. 514–517.

[3] I. BABUSKA I AND M. SURI, *Locking effects in the finite element approximation of elasticity problems*, Numer. Math., 62 (1992), pp. 439–463.

[4] K. BELL, *A refined triangular plate bending element*, Int. J. Numer. Methods. Engrg., 1 (1969), pp. 101–122.

[5] L. J. BILLERA, *Homology of smooth splines: generic triangulations and a conjecture of Strang*, Trans. AMS., 310 (1988), pp. 325–340.

[6] H. BLUM AND R. RANNACHER, *On the boundary value problem of the biharmonic operator on domains with angular corners*, Math. Meth. Appl. Sci., 2 (1980), pp. 556–581.

[7] S. C. BRENNER AND L. R. SCOTT, The Mathematical Theory of Finite Element Methods, Springer-Verlag, New York, 1994.

[8] S. C. BRENNER AND L.-Y. SUNG, *C_0 interior penalty methods for fourth order elliptic boundary value problems on polygonal domains*, J. Sci. Comput., 22/23 (2005), pp. 83–118.

[9] F. K. BOGNER, R. L. FOX AND L. A. SCHMIT, *The generation of interelement compatible stiffness and mass matrices by the use of interpolation formulas*, Proceedings of the Conference on Matrix Methods in Structural Mechanics, Wright Patterson A.F.B. Ohio, 1965.

[10] P. G. CIARLET, The Finite Element Method for Elliptic Problems, North-Holland, Amsterdam, 1978.

[11] R. W. CLOUGH AND J. L. TOCHER, *Finite element stiffness matrices for analysis of plates in bending*, Proceedings of the Conference on Matrix Methods in Structural Mechanics, Wright Patterson A.F.B. Ohio, 1965.

[12] J. DOUGLAS JR., T. DUPONT, P. PERCELL AND R. SCOTT, *A family of C^1 finite elements with optimal approximation properties for various Galerkin methods for 2nd and 4th order problems*, RAIRO. Anal. Numer., 13 (1979), pp. 227–255.

[13] A. EL-ZAFRANY AND R. A. COOKSON, *Derivation of Lagrangian and Hermitian shape functions for quadrilateral elements*, Int. J. Numer. Methods. Engrg., 23 (1986), pp. 1939–1958.

[14] B. FRAEUS DE VEUBEKE, *Bending and stretching of plates*, Proceedings of the Conference on Matrix Methods in Structural Mechanics, Wright Patterson A.F.B. Ohio, 1965.

[15] B. FRAEUS DE VEUBEKE, *A conforming finite element for plate bending*, Stree Analysis, O.C. Zienkiewicz and G. S. Holister ed. 1965, Wiley, New York, pp. 145–197.

[16] V. GIRAULT AND L. R. SCOTT, *Hermite interpolation of nonsmooth functions preserving boundary conditions*, Math. Comp., 71 (2002), pp. 1043–1074.

[17] S. GOPALACHARYULU, *A higher order conforming, rectangular plate element*, Int. J. Numer. Methods Engrg., 6 (1973), pp. 305–308.

[18] S. GOPALACHARYULU, *Author's reply to the discussion by Watkins*, Int. J. Numer. Methods. Engrg., 6 (1976), pp. 471–472.

[19] P. GRISVARD, Elliptic Problems in Nonsmooth Domains, Pitman Pub. Inc., 1985.

[20] Z. C. LI AND N. YAN, *New error estimates of bi-cubic Hermite finite element methods for biharmonic equations*, J. Comp. Appl. Math., 142 (2002), pp. 251–285.

[21] S. P. MAO, The Theory and Applications of Anisotropic Finite Element Methods (in Chinese), Ph.D. Thesis, Chinese Academy of Sciences, 2008.

[22] J. MORGAN AND L. R. SCOTT, *A nodal basis for C^1 piecewise polynomials of degree n*, Math. Comp., 29 (1975), pp. 736–740.

[23] J. MORGAN AND L. R. SCOTT, *The dimension of the space of C^1 piecewise-polynomials*, Research Report UH/MD 78, Dept. Math., Univ. Houston, 1990.

[24] P. OSWALD, *Multilevel preconditioners for discretizations of the biharmonic equation by rectangular finite elements*, Numer. Lin. Alg. Appl., 6 (2005), pp. 487–505.

[25] P. PERCELL, *On cubic and quartic Clough-Tocher finite elements*, SIAM J. Numer. Anal., 13 (1976), pp. 100–103.

[26] J. PETERA AND J. F. T. PITTMAN, *Isoparametric Hermite elements*, Int. J. Numer. Methods. Engrg., 37 (1994), pp. 3489–3519.

[27] M. J. D. POWELL AND M. A. SABIN, *Piecewise quadratic approximations on triangles*, ACM Trans. Math. Software., 3–4 (1977), pp. 316–325.

[28] G. SANDER, *Bornes supérieures et inférieures dans l'analyse matricielle des plaques en flexion-torsion*, Bull. Sco. Roy. Sci. Liège., 33 (1964), pp. 456–494.

[29] L. R. SCOTT AND M. VOGELIUS, *Norm estimates for a maximal right inverse of the divergence operator in spaces of piecewise polynomials*, RAIRO, Model. Math. Anal. Numer., 19 (1985), pp. 111–143.

[30] L. R. Scott and M. Vogelius, *Conforming finite element methods for incompressible and nearly*

incompressible continua, Lect. Appl. Math., 22 (1985), pp. 221–244.

[31] L. R. SCOTT AND S. ZHANG, *Finite element interpolation of nonsmooth functions satisfying boundary conditions* , Math. Comp., 54 (1990), pp. 483–493.

[32] R. STENBERG AND M. SURI, *Mixed hp finite element methods for problems in elasticity and Stokes flow*, Numer. Math., 72 (1996), pp. 367–389.

[33] G. STRANG, *Piecewise polynomials and the finite element method*, Bull. AMS., 79 (1973), pp. 1128–1137.

[34] G. STRANG, *The dimension of piecewise polynomials, and one-sided approximation*, in "Conf. on Numerical Solution of Differential Equations", Lecture Notes in Mathematics 363, G. A. Watson ed., Springer-Verlag, Berlin, 1974, pp. 144–152.

[35] L. B. WAHLBIN, Superconvergence in Galerkin Finite Element Methods, Lect. Notes. Math., Vol. 1605, Springer, Berlin, 1995.

[36] D. S. WATKINS, *A comment on Gopalacharyulu's 24 node element*, Int. J. Numer. Methods. Engrg., 6 (1976), pp. 472–474.

[37] S. ZHANG, *An optimal order multigrid method for biharmonic, C^1 finite-element equations*, Numer. Math., 56 (1989), pp. 613–624.

[38] S. ZHANG, *A family of $Q_{k+1,k} \times Q_{k,k+1}$ divergence-free finite elements on rectangular grids*, SIAM J. Num. Anal., 47 (2009), pp. 2090–2107.

[39] S. ZHANG, *A divergence-free finite element method for the 3D Navier-Stokes equations in the vorticity-vector potential form*, 2009, preprint.